

A HISTORICAL AND CURRENT PERSPECTIVE ON PREDICTING THERMAL COOKOFF BEHAVIOR

A. K. Burnham*, R. K. Weese, A. P. Wemhoff and J. L. Maienschein

Energetic Materials Center, Lawrence Livermore National Laboratory, Livermore, CA 94550, USA

Prediction of thermal explosions using chemical kinetic models dates back nearly a century. However, it has only been within the past 25 years that kinetic models and digital computers made reliable predictions possible. Two basic approaches have been used to derive chemical kinetic models for high explosives: [1] measurement of the reaction rate of small samples by mass loss (thermogravimetric analysis, TG), heat release (differential scanning calorimetry, DSC), or evolved gas analysis (mass spectrometry, infrared spectrometry, etc.) or [2] inference from larger-scale experiments measuring the critical temperature (T_m , lowest T for self-initiation), the time to explosion as a function of temperature, and sometimes a few other results, such as temperature profiles. Some of the basic principles of chemical kinetics involved are outlined, and major advances in these two approaches through the years are reviewed.

Keywords: chemical kinetics, energetic materials, explosives, thermal explosions, thermal ignition

Approaches to chemical kinetics

Thermal explosions are caused by runaway exothermal chemical reactions. The reaction starts to accelerate if the rate of heat dissipation falls behind the rate of heat generation. The rate of heat generation increases exponentially with temperature, while the rate of heat dissipation increases only linearly with temperature. A thermal explosion will then result if the enthalpy of the exothermic reaction is sufficiently great to heat the material to hundreds or thousands of degrees in a fraction of a second along with the generation of a significant amount of gaseous product.

The usual starting point for thermal explosions is the Arrhenius equation

$$k = Ze^{-E/RT} \quad (1)$$

where k is the rate constant, Z is a frequency factor, and E is an activation energy. Essentially all chemical processes of interest contain multiple elementary chemical reactions, hence multiple rate constants. For thermal decomposition, the overall reaction is typically a combination of initiation, propagation, and termination (recombination) free-radical reactions. Initiation reactions are usually endothermic, and for energetic materials, the others are usually exothermic.

A variety of chemical rate laws have been considered for thermal decomposition. The simplest and most common is an n^{th} -order reaction for one material A converted to another material B:

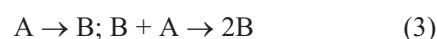
$$dA/dt = -dB/dt = -kA^n; \quad (2)$$

$$d(1 - \alpha)/dt = -k(1 - \alpha)^n$$

where α is the fractional conversion and n is the reaction order. If $n=0$, the reaction rate depends only on temperature and not the extent of reaction. A unimolecular decomposition reaction has $n=1$, or first order, and both the reaction rate and amount of initial material will decay exponentially with time. If $n>1$, the reaction rate will initially decrease faster with time than a first-order reaction but extend to longer time.

Energetic materials and thermal explosions are commonly linked with induction times, or a time where little happens before the system heats rapidly and feeds back on itself catastrophically. There are actually two separate induction time phenomena – one chemical and one thermal. The former involves a vigorously acceleratory chemical reaction at constant temperature, and the latter is an exponentially increasing reaction rate due to increasing temperature.

There are several simple and related acceleratory mechanisms related to the reaction sequences



The relevant differential equation is

$$\begin{aligned} dA/dt &= -k_1A - k_2AB; \\ d\alpha/dt &= k_1(1 - \alpha)^{n_1} + k_2\alpha^m(1 - \alpha)^{n_2} \end{aligned} \quad (4)$$

* Author for correspondence: burnham1@llnl.gov

Here we have added empirical reaction orders to each of the conversion terms in Eq. (4). They would be unity if Eq. (3) were rigorously correct, but they serve a useful purpose in empirical model fitting. Equation (4) is often simplified by assuming that $n_1=n_2$, giving

$$\begin{aligned} d\alpha/dt &= k_2(1-\alpha)^n (\alpha^m + z) \approx \\ &\approx k_2(1-\alpha)^n (1-q(1-\alpha))^m \end{aligned} \quad (5)$$

where $z=k_1/k_2 \approx 1-q$. The left-hand side is used in the CISP software [1], and the right-hand side of Eq. (5) has been called the extended Prout–Tompkins model [2]. For $m=0$, Eq. (5) reduces to an n^{th} -order reaction, and for $n=0$, it reduces to a linear chain-branching reaction. Consequently, Eqs (4) and (5) contain the basic characteristics of sequential reactions as well as reactions that can undergo extremely rapid acceleration for $m>1$.

Numerous thermal analysis experiments on many explosives shown that energetic materials are intrinsically autocatalytic, and the reaction profiles are narrower than predicted by a first-order reaction with an activation energy derived by Kissinger's method. Consequently, Eq. (5) provides the minimum complexity of chemical reaction model needed to model energetic materials, and early kinetic parameters derived using Eq. (2) should be discarded as unreliable. However, most energetic materials have a reaction profile that is more complex than a single reaction profile consistent with Eq. (5). This can be addressed by one of three approaches:

- Develop more detailed mechanism than Eq. (3).
- Construct empirical models from multiple extended Prout–Tompkins reactions, and
- Use an advanced isoconversional kinetic approach, in which an activation energy is derived for each small portion of reaction (1% in α or less) and they react sequentially.

Option 1 includes a range of possibilities from relatively small reaction networks within the range of Netzsch [3] and CISP [1] software to full-blown detailed reaction mechanism involving hundreds of reactions [4]. Other progress along the lines of option 1 has been obtained by computer simulations of the decomposing molecules [5]. Other work seeks to develop simplified mechanistic models that are more rigorous than the global models but not as detailed as those that have been developed for combustion models [6]. Although very promising, these more fundamental models are still in the early stages of development and will not be covered in detail here. Moreover, they are typically out of the scope of thermal analysis.

Option 2 assumes that individual features of the reaction profile are independent of each other. One could either fit a small number of concurrent reactions with Z and E determined specially for each feature, or one could fit a large number of parallel reactions analogously to the discrete activation energy distribution model used extensively in petroleum geochemistry by assuming only a single Z factor or one with a prescribed functional relationship to E . Determining Z and E for each feature individually allows the reaction profile to change shape as a function of heating rate. The danger, however, is that if the reactions really have sequential characteristics, the model can erroneously predict that two reactions will switch order. Independent evidence is needed to determine whether such a switch is correct or not.

Option 3 is an enhancement of the basic isoconversional approaches of differential Friedman [7] and integral Ozawa–Flynn–Wall [8]. They received a resurgence in recent years in the thermal analysis community due to the efforts of Vyazovkin [9], who improved the integral approach. They are also available in kinetics analysis software packages from Mettler-Toledo, Netzsch, AKTS [10], and LLNL. The basic premise of the differential approach [11], which we use, is that Z and E can be determined at any selected fraction converted, α , for a set of experiments with different thermal histories using a simple Arrhenius plot:

$$\ln(-d(1-\alpha)/dt) = -E/RT + \ln(Z(1-\alpha))$$

Advanced isoconversional methods represent the limit of a sequential model in which the reaction interval covered by each segment approaches zero. The form factor of the reaction is absorbed into the conversion dependence of an effective Z value. As such, the resulting model is the best that can be done for systems that are sequential in character. It also works for systems in which the reaction characteristics are concurrent but for which the activation energy increases with the extent of conversion. Because it works well in these two limits, it is probably the best bet for systems that are complex and not well characterized. However, it does contain assumptions that may not be valid and should not be believed blindly.

Approaches to thermal modeling

The earliest attempts to combine exothermic chemical reaction rates with heat loss date back to the early 20th century. The Frank–Kamenetskii and associated equations are outlined by Merzhanov and Abramov [11]. Assuming a zero-order reaction, the

lowest temperature, T_m , at which a piece of explosive placed in a heat bath will thermally ignite is given by,

$$T_m = (E/R)/\ln(ZE\Delta H\tau/C_pRT_m^2\delta) \quad (6)$$

where ΔH is the heat of reaction, τ is r^2/λ , where r is the radius of a sphere or infinite cylinder and λ is the thermal diffusivity, C_p is the specific heat, and δ is a dimensionless factor equal to 3.32 for spheres, 2.00 for cylinders, and 0.88 for slabs. Equation (6) must be solved iteratively for T_m .

The time to explosion for adiabatic conditions (initially at uniform temperature and perfectly insulated) as a function of temperature is given by

$$t_{\text{exp}} = (C_pRT^2/ZE\Delta H)e^{-E/RT} \quad (7)$$

When the sample is initially at room temperature and is then plunged into a heat bath, the explosion time will be longer due to the time for heat to diffuse into the sample. The time to explosion then becomes

$$t_{\text{exp}} = (\rho C_p/\lambda)\delta r^2 E(1/T_m - 1/T) \quad (8)$$

where ρ is the density and λ is the thermal conductivity. Here, the time to explosion is proportional to the distance from the critical temperature in reciprocal temperature space. However, it should be noted that Eq. (8) is an approximation, and for finite objects, T_m actually depends on λ , so the situation is more complicated.

Although Eqs (6)–(8) are interesting from a historical and educational perspective, they involve assumptions now known to be not very good, so there is really no reason for their continued use in the age of modern digital computing. Numerous computer programs, some commercial, some proprietary, can accurately integrate the relevant differential equations for more realistic chemical kinetic models and thermal transport properties that vary with temperature, and in some cases, fraction converted.

A few curves showing the dependence of explosion time on size and shape are shown in Fig. 1 for a first-order and Prout–Tompkins ($m=1$, $q\approx 1$) reactions. Calculations used the AKTS Thermal Safety program [10]. Both reactions have calculated maximum reaction rates at typical thermal analysis conditions of 0.1, 1 and 10°C min⁻¹ of 216, 244 and 275°C, respectively. The difference is the first-order reaction is much broader (FWHH=31°C vs. 2°C). The practical effect of this difference is that the Prout–Tompkins reaction is not particularly sensitive to thermal diffusion of generated heat, because the reaction accelerates rapidly after the chemical kinetic induction period. This gives a result much closer to the adiabatic limit and a much lower critical temperature and longer critical time. Both reaction types are susceptible at high external temperatures to

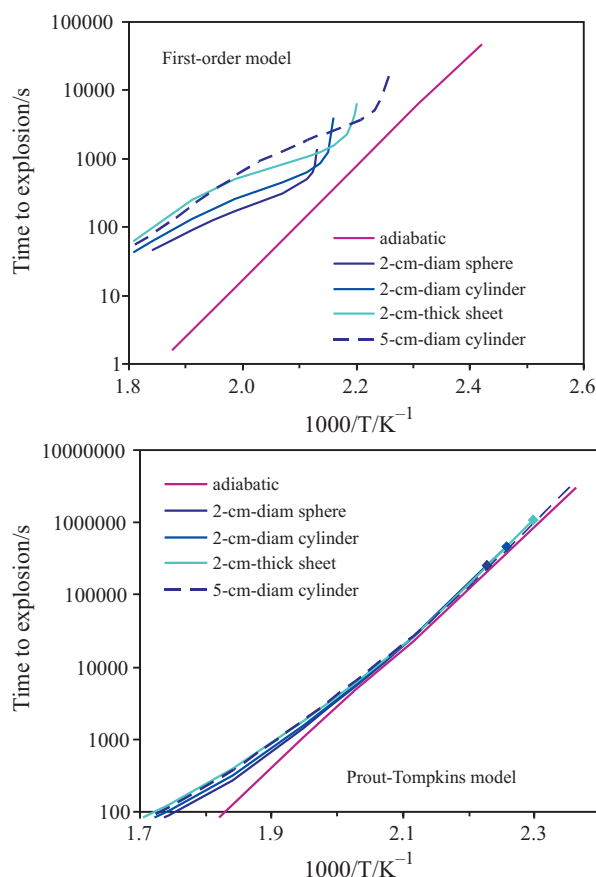


Fig. 1 Dependence of the explosion time and critical temperature on shape and size for a first-order and Prout–Tompkins reactions having activation energies of 167.36 kJ mol⁻¹. The frequency factor Z is $1 \cdot 10^{14}$ s⁻¹ for the first-order reaction and $2.5 \cdot 10^{15}$ s⁻¹ and for the P–T reaction. All calculations used $\Delta H = -4184$ kJ g⁻¹, $\rho = 1.778$ g cm⁻³, λ of 0.0015 W cm⁻¹ K⁻¹, C_p of 1.5 J g⁻¹ K⁻¹, and an external heat transfer coefficient of 0.1 W cm⁻² K⁻¹

the heat transfer coefficient, which is moderate in this case. Also worth noting is that the adiabatic explosion time has an apparent activation energy of 159 kJ mol⁻¹, which is close to, but not equal to, the simulation value. In contrast, the finite bodies undergoing a first-order reaction have a lower apparent value over any given temperature range due to the combination of chemical kinetic and heat-diffusion contributions. The upturns at low temperature are characteristic of reactions with a low degree of autocatalytic character.

Optimizing kinetic models for thermal explosion prediction

Kinetic models can be calibrated either by (1) measurement of the reaction rate of small samples by mass loss (thermogravimetric analysis, TG), heat release

(differential scanning calorimetry, DSC), or evolved gas analysis (mass spectrometry, infrared spectrometry, etc.) or (2) inference from larger-scale experiments measuring the critical temperature (T_m , lowest T for self-initiation), the time to explosion (t_{exp}) as a function of T , and sometimes a few other results, such as temperature profiles.

The first approach has the advantage that aspects of the reaction can be isolated and quantified in detail. Also, if the experiments are done carefully, the decomposition reactions occur at a well defined temperature and pressure. However, it has had variable success at reliably predicting thermal explosion temperatures for macroscopic pieces of high explosive, particularly when used to derive kinetic rate constants to be used in one-dimensional codes combining heat transfer and chemical kinetics. Consequently, any kinetic parameters derived by this approach should only obtain credence by their ability to match larger-scale integrated experiments.

As a starting point, various measures of thermal stability are cross-plotted in Fig. 2 to determine mutual relationships for various explosive formulations of HMX, RDX, TNT, PETN, and double-base materials [12]. Within the context of thermal analysis, a simple linear correlation between DSC T_{max} in a closed pan at 6°C h^{-1} and macroscopic thermal explosion experiments could predict these cookoff temperatures to about $\pm 10^\circ\text{C}$. DSC decomposition temperatures under conventional conditions ($10^\circ\text{C min}^{-1}$, open pan) did not correlate particularly well with cookoff temperatures from these larger-scale experiments. At the same heating rate, the 1/4" cylinders ignited about 20°C lower than the DSC T_{max} , which is in the vicinity of the onset of decomposition in the DSC. HMX materials lie on average about 15°C below the trend of the other materials, which suggests that decomposition kinetics for stronger confinement are faster than in a DSC closed pan. The best correlation is between the thermal explosion temperatures for a 2" cylinder heated at 1°C h^{-1} (STEX) and a 1/4" cylinder heated at 6°C h^{-1} (mini-STEX), with the latter tending to be about 10°C higher.

Derivation of decomposition kinetics for energetic materials for the purpose of predicting thermal explosions is now common, and Roduit [10] has claimed great success scaling from mg to Mg scales. However, his work has looked at a relatively narrow range of materials. Our experience is that kinetics from DSC sometimes simulate larger-scale experiments well and sometimes not. Figure 3 shows a comparison of measured and predicted ODTX results for HMX, which we have studied the most. Our HMX decomposition kinetics were measured in

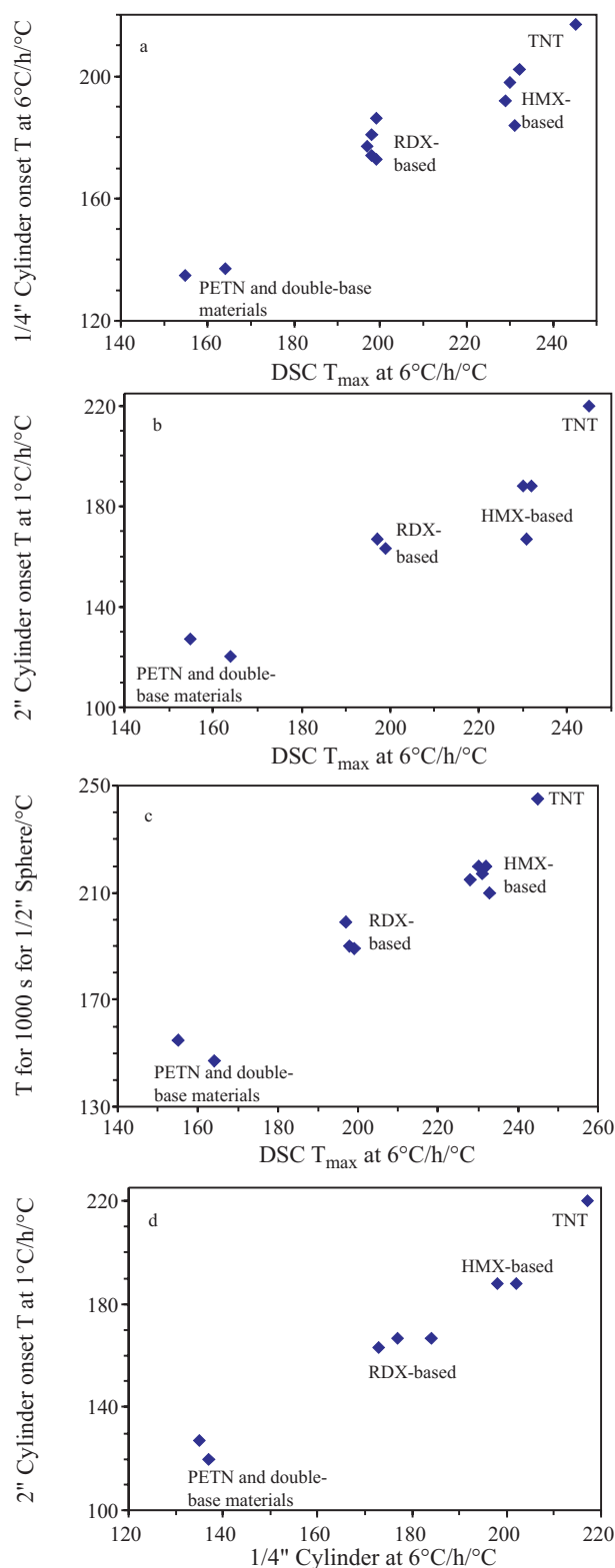


Fig. 2 Cross-comparison of various measures of thermal stability. DSC in closed pans correlates fairly well with macroscopic thermal explosion experiments, but the best correlation is between 1/4" and 2" cylinders

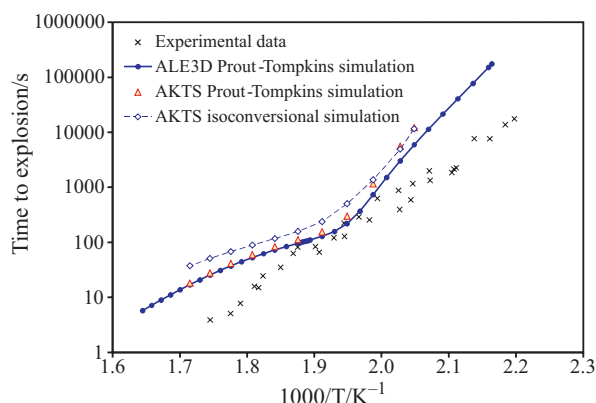


Fig. 3 A comparison of ODTX measurements and calculations using isoconversional and extended Prout–Tompkins models in the AKTS Thermal Safety program and the extended Prout–Tompkins model in the LLNL ALE3D computer program. The P–T parameters are $Z=3.81 \cdot 10^{13} \text{ s}^{-1}$, $E=164.42 \text{ kJ mol}^{-1}$, $n=0.320$, $m=0.635$ and $q=0.99$

hermetically sealed pans and were reported at NATAS two years ago. Predictions are nearly identical for isoconversional and extended Prout–Tompkins models as well as from the LLNL ALE3D code and the AKTS Thermal Safety code. The difference between the two codes was subsequently traced to a difference in the thermal properties of the gas assumed by ALE3D, since it is a multiphase code while the AKTS code is a single phase. We will return to a comparison of DSC and macroscopic thermal explosion experiments in a later section.

Probably the most successful approach at predicting large-scale thermal explosions is due to Tarver and coworkers, who developed simple sequential and autocatalytic kinetic models for a variety of explosives over the past 25 years [13–17]. The approach assumes temperature-dependent thermal properties of both the solid and gas phases, uses activation energies similar to those in more complicated mechanisms, and optimizes the kinetic parameters against ODTX experiments. Some of the kinetic parameters from Tarver and coworkers are summarized in Table 1, and a few comparisons of measurement and calculations are shown in Figs 4 and 5. Of potential interest in Fig. 5 is the dependence of explosion time on confinement pressure. Despite the impressive model-calculation comparisons in Figs 4 and 5, there are discrepancies that still need to be resolved. Kaneshige [18] found that the original Tarver-McGuire HMX and PBXN-109 kinetics [14] predict too slow an ignition time the SNL’s SITI experiment. Furthermore, there are questions of uniqueness of the kinetic parameters and how they are affected by uncertainty in the thermal properties.

Table 1 Summary of thermal explosion models for various explosives using the approach of Tarver and coworkers [12–16]

Reaction	$\ln Z$	$E/\text{kJ mol}^{-1}$	$\Delta H/\text{J g}^{-1}$
HMX: coarse ^a and fine ^b			
A→B	48.7	216.3	+251
B→2C	37.8 ^a 38.2 ^b	185.4	−556.6
2C→D	28.1 ^a 28.5 ^b	142.7	−5594
RDX			
A→B	45.5	197.1	+418
B→2C	40.7	184.5	−1255
2C→D	35.0	142.7	−5021
TNT			
A→B	57.0	270.2	+209.2
B→C	52.8	249.4	+209.2
C+C→D	37.5	184.1	−3765
PETN			
A→B	45.59	196.6	+209.2
A+B→C	41.95	178.3	−523.0
B+B→C	36.00	149.7	−627.6
C+C→D	32.00	126.8	−5439.2
Nitrocellulose			
A→B	36.0	182.8	+104.6
B→C	28.8	144.8	−3564.8
TATB			
A→B	29.5	175.7	209.2
A+B→C	45.0	251.0	−3766
B+B→C	45.0	251.0	−3975

Erikson [19] proposed that simpler kinetic models traditionally used by the thermal analysis community could be optimized directly against the ODTX data. He explored the shape of the curve relating explosion time to reciprocal temperature and concluded that acceleratory (linear and 3/2 power branching reactions) and sigmoidal (cubic autocatalysis) reactions reproduced the linear relationship typically observed, while other reaction models had bends in the relationship that are not generally observed. He also had good success predicting explosion times for HMX using isoconversional kinetics from Lofy and Wight [20] as long as he increased their frequency factor tenfold.

We have extended this approach for a variety of explosives using the extended Prout–Tompkins model, Eq. (5), which contains the three acceleratory and sigmoidal models favored by Erikson as limits.

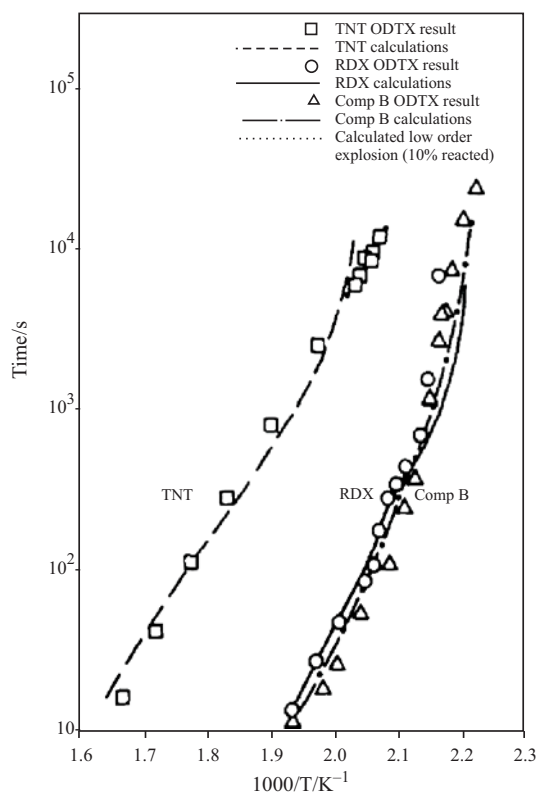


Fig. 4 Comparison of measured and calculated ODTX experiments from McGuire and Tarver (1981)

The first step is to understand how the different parameters affect the shape of the curve. Parametric studies are shown in Fig. 6. The parameters q and m affect the straightness of the curve and interact with each other. Physically, $1-q$ is the ratio of the initiation (nucleation) and propagation (growth) rate constants, while m is the dimensionality of growth. When $q \approx 1$ and $m=1$ (Prout–Tompkins ($n=1$) and linear chain-branching ($n=0$) limits), the relationship between the logarithm of explosion time and reciprocal temperature is nearly linear. When $q=0.99$, the curve for $m=1$ has a definite kink at about $1000/T=2.08$ K for this Z and E . As q becomes closer to unity, a greater compensating increase in Z is required to maintain the same explosion time at high temperature. The reaction order n has little effect except near the critical temperature. The $n=1$ explosion time increases more sharply than for $n=0$ near the critical temperature as m decreases. It is most pronounced in the first-order limit ($n=1, m=0$) as also seen in Fig. 1. In all cases, the critical temperature (end of line) is lower for $n=1$ than $n=0$. This result shows the difficulty of predicting the critical temperature accurately from higher T ODTX data by this curve fitting method and points out the need for long time (multiple days) cookoff experiments.

Parameters were optimized manually using the AKTS Thermal Safety program and by a stepwise

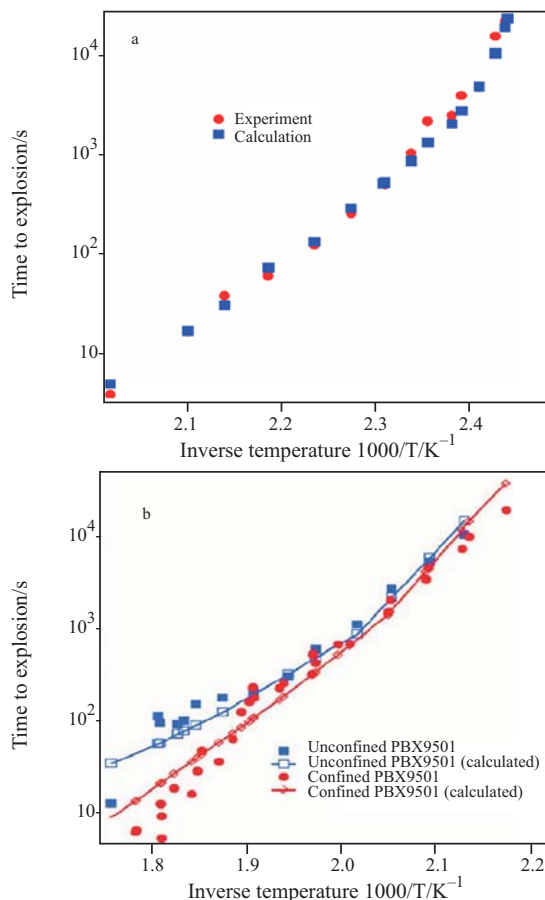


Fig. 5 Comparison of measured and calculated ODTX experiments for a – PETN and b – an HMX formulation. The difference between confined PBX9501 indicates that pressure can affect the decomposition kinetics

numerical procedure using the LLNL ALE3D program. The latter optimization used a representative subset of the data and the LLNL optimization code Global Local Optimizer (GLO), which minimized the square of the difference between the logarithms of measured and calculated explosion times using the method of steepest descents. The results of this approach are shown in Fig. 7 for HMX and PETN.

Once kinetic parameters are derived from ODTX, one can ask the reverse question on how well they predict the DSC experiments. This is shown in Fig. 8 for HMX and PETN. For both materials, the ODTX kinetics predict a similar onset temperature to what is observed but also predict that the reaction accelerates much more quickly to the peak reaction rate and completion.

Based on evidence that the time to explosion increases in the ODTX apparatus, we have suspected for some time that degree of autocatalysis depends strongly on confinement conditions. Consequently, we procured and recently instituted high-pressure

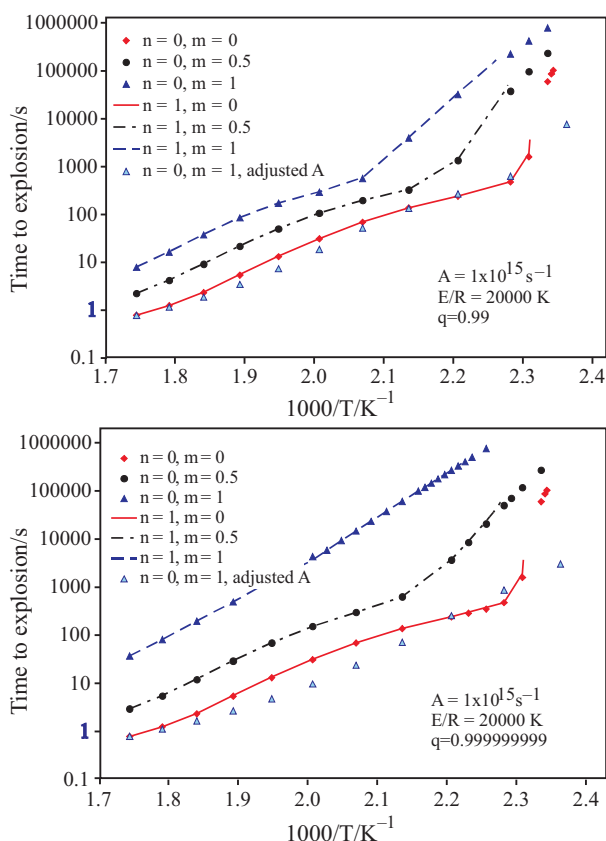


Fig. 6 Dependence of time vs. $1/T$ relationship on parameters of the extended Prout–Tompkins model. The adjusted Z values were 57 times larger for $q=0.99$ and 1000 times larger for $q=0.999999999$

DSC. Experiments were conducted in thin, crimped pans with minimal internal volume so that the gas composition inside the pan is largely self-generated while the pressure inside the pan is determined by the external pressure. Initial results for HMX are shown in Fig. 9. Pressure clearly accelerates and sharpens the decomposition reaction.

Figure 10 shows the dependence of heat flow on heating rate at 1000 psi. The heat flow curves approach those in Fig. 8 (top). The confining pressure in the ODTX experiment is 20 times higher (150 MPa) that our highest DSC pressure, and since T_{\max} in Fig. 9 decreases linearly with the logarithm of pressure, one would expect the curves to shift another 15°C or so lower in temperature, which puts them in excellent agreement with Fig. 8. Kinetic parameters derived using Eq. (5) are $A=2.83\cdot 10^{12}\text{ s}^{-1}$, $E=140.7\text{ kJ mol}^{-1}$, $m=1.17$, $n=0.71$ and $q=0.9999$. Due to the strong induction character reflected in these parameters, it was important to start the numerical integration at least 50°C below the decomposition temperature for proper convergence. The activation energy is within the uncertainty of the

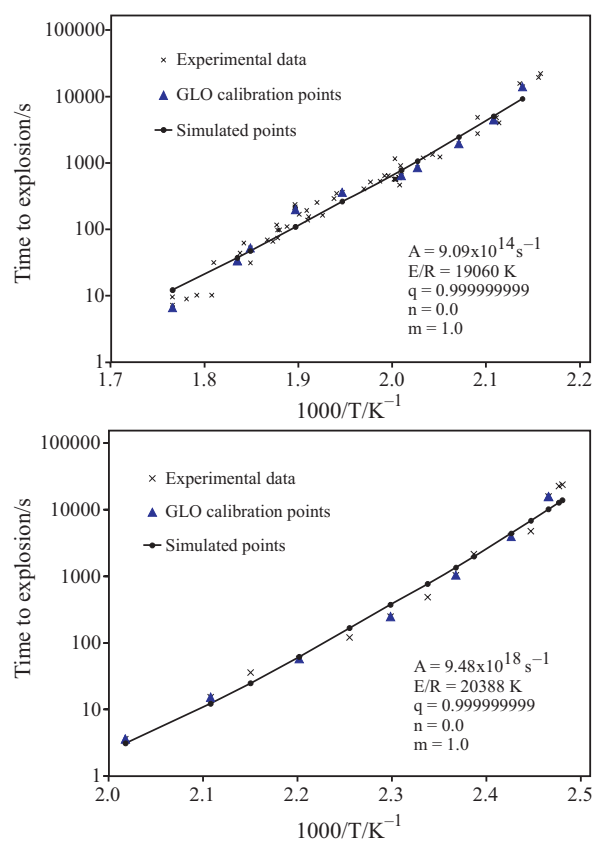


Fig. 7 Fits of a – HMX and b – PETN ODTX data to the extended Prout–Tompkins model

atmospheric pressure value and only a little lower than inferred directly from ODTX in Fig. 7 (top).

The shift in T_{\max} is consistent with a $P^{0.3}$ dependence of the reaction rate. Extrapolation to 150 MPa is accomplished by increasing A to $8\cdot 10^{12}\text{ s}^{-1}$ to decrease T_{\max} by another 15°C . However, this does not account for the change in profile shape. The relative constancy of the onset temperature with an acceleration of the subsequent reaction process is consistent with autocatalysis and other bimolecular reactions typical of the simplified mechanisms in Table 1. It may be possible to mimic this mechanistic effect in an isoconversional kinetic approach by having the pressure dependence be a function of conversion. The pressure dependence is consistent with Fig. 5 (bottom) but superficially inconsistent with other pressure experiments [21, 22] that show HMX and RDX decomposition to be decelerated by increased pressure near the GPa range. Cage effects are probably dominant in the GPa pressure range.

The cookoff predictions using the high-pressure DSC kinetics agree much better with the ODTX data than the atmospheric pressure kinetics, as shown in Fig. 11. The calculated curve is much straighter, which is due to q being closer to unity. The DSC activation energy appears to be a little low. However,

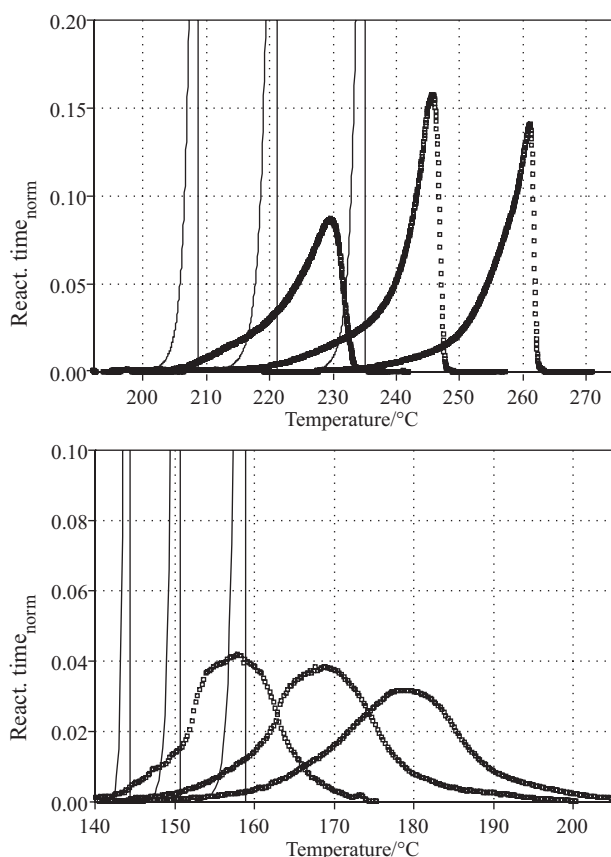


Fig. 8 Comparison of observed heat release from DSC experiments (points) using a – HMX and b – PETN heated at 0.1, 0.35, and 1.0°C min⁻¹ (from left to right) with that calculated (thin lines) from the kinetics optimized on the ODTX experiments using ALE3D. The melt endotherm occurs at 138°C for PETN in this data

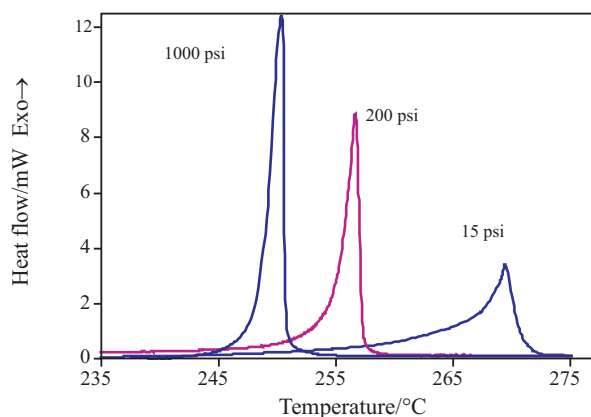


Fig. 9 Comparison of HMX heat release curves as a function of pressure at a heating rate of 1.0°C min⁻¹

given the amount of extrapolation required from highest DSC pressure, the agreement is quite good for an initial effort.

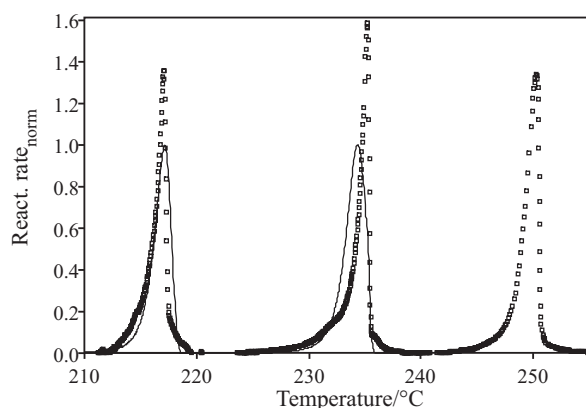


Fig. 10 Heat release curves as a function of heating rate (0.10, 0.35, and 1.0°C min⁻¹ from left to right) at 1000 psi pressure

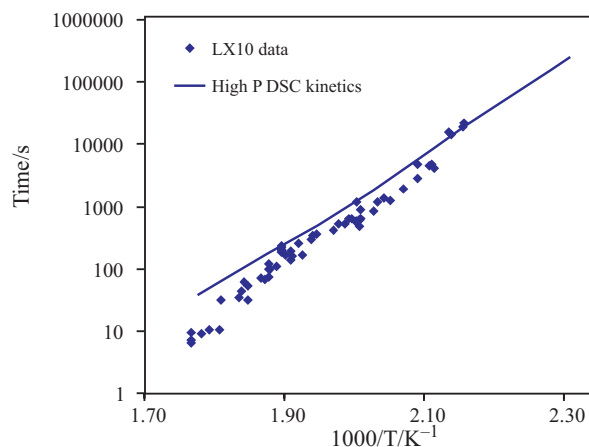


Fig. 11 Comparison of measured ODTX results for LX-10 with those calculated using extended Prout–Tompkins kinetics derived from high-pressure DSC experiments

Conclusions

Although early treatments of thermal explosions, such as the Frank–Kamenetskii equation, contain the important aspect of the competition between heat generation and heat dissipation, they are fundamentally flawed by the simplified chemical kinetic models employed. Decomposition of energetic materials have acceleratory or sigmoidal kinetics, which reflect the sequential nature of the reaction mechanism. In addition, the reaction progress depends heavily on confinement conditions, which influences the course of secondary reactions between products with themselves and initial material. Tarver *et al.* successfully combined simple sequential reaction mechanisms with heat transfer calculations to accurately simulate ODTX and related cookoff experiments. More recently, we have had good success fitting an extended Prout–Tompkins model directly to ODTX results. In contrast, kinetics derived

from thermal analysis experiments have had limited success with predicting the results of these larger-scale experiments. Part of the problem is that, years ago, inappropriate deceleratory (n^{th} -order) models were used to analyze the thermal analysis data. More recently, kinetics analysis programs have simplified the calibration of appropriate kinetic parameters, such as isoconversional and extended Prout–Tompkins models. Both these approaches have the sequential character needed for energetic material decomposition. Even so, these kinetic parameters do not reliably predict large-scale cookoff experiments unless the thermal analysis experiments are conducted under appropriate confinement conditions. Roduit and coworkers have had good success using sealed, thick DSC pans, but it is not yet known how generally they will work. We have had excellent success with HMX using thin sealed pans and an external pressuring gas. Although there are still details to be worked out, future prospects are bright for using thermal analysis experiments to predict large-scale thermal explosion phenomena.

Acknowledgements

This work was performed under the auspices of the U.S. Department of Energy by the University of California, Lawrence Livermore National Laboratory, under Contract No. W-7405-Eng-48.

References

- 1 Cheminform, St. Petersburg Ltd. (CISP) 197198, 14 Dobrolubov Ave., Saint-Petersburg, Russia.
- 2 A. K. Burnham, *J. Therm. Anal. Cal.*, 60 (2000) 895.
- 3 Netzsch-Gerätebau, Wittelsbacherstrasse 42, D-95100 Selb/Bavaria, Germany.
- 4 C. F. Melius, in *Chem. and Phys. of Energet. Mater.*; Bulusu, S. N., Ed.; Kluwer: Dordrecht (1990) pp. 51–78.
- 5 M. R. Manaa, L. E. Fried, C. F. Melius, M. Elstner and T. Fraunheim *J. Phys. Chem. A*, 106 (2002) 9024.
- 6 S. Maharrey and R. Behrens, Jr., *J. Phys. Chem. A.*, 109 (2005) 11236.
- 7 H. L. Friedman, *J. Polym. Sci. C*, 6 (1964) 183.
- 8 J. H. Flynn, *Thermochim. Acta*, 282/283 (1996) 35.
- 9 S. Vyazovkin, *J. Comput. Chem.*, 22 (2001) 179.
- 10 B. Roduit, C. Borgeat, B. Berger, P. Folly, B. Alonso and J. N. Aebischer, *J. Therm. Anal. Cal.*, 80 (2005) 91.
- 11 A. G. Merzhanov and V. G. Abramov, *Prop. Expl.*, 6 (1981) 130–148.
- 12 A. K. Burnham, R. K. Weese, J. F. Wardell, T. D. Tran, A. P. Wemhoff and J. L. Maienschein, 13th Int. Det. Symp., July, 2006.
- 13 C. M. Tarver, R. R. McGuire, E. L. Lee, E. W. Wrenn and K. R. Brein, 17th Symp. Int. on Combustion, (1978) pp. 1407–1413.
- 14 R. R. McGuire and C. M. Tarver, *Proc. 7th Symp. Int. on Detonation*, (1981) pp. 56–64.
- 15 C. M. Tarver and T. D. Tran, *Combust. Flame*, 137 (2004) 50.
- 16 C. M. Tarver and T. D. Tran, *Prop. Expl. Pyro.*, 28 (2004) 189.
- 17 J. J. Yoh, M. A. McClelland, J. L. Maienschein, J. F. Wardell and C. M. Tarver, *J. Appl. Phys.*, 97 (2005) 083504-1-11.
- 18 M. J. Kaneshige, A. M. Renlund, R. G. Schmidt and W. W. Erikson, 12th Int. Det. Symp., San Diego, ONR 333-05-2 (2002) pp. 821–830.
- 19 W. W. Erikson, Application of global decomposition models to energetic material cookoff, JANNAF 40th CS, 28th APS, 22nd PSHS, and 4th MSS Joint Meeting, Charleston, SC, June 2005.
- 20 P. Lofy and C. A. Wight, JANNAF 35th Combustion Subcommittee and 17th Propulsion Systems Hazards Subcommittee Meeting, CPIA Pub. 685 (1998) pp. 137–143.
- 21 E. L. Lee, R. H. Sanborn and H. D. Stromberg, *Proc. 5th Symp. (Int.) on Detonation*, (1970) p. 331.
- 22 G. J. Piermarini, S. Block and P. J. Miller, *J. Phys. Chem.* 91 (1989) 3872–3878.

DOI: 10.1007/s10973-006-8161-6